EJN European Journal of Neuroscience

FENS Federation of European Neuroscience Societies

European Journal of Neuroscience, Vol. 42, pp. 2851–2859, 2015 doi:10.1111/ejn.13063

COGNITIVE NEUROSCIENCE

Decoding sequential finger movements from preparatory activity in higher-order motor regions: a functional magnetic resonance imaging multi-voxel pattern analysis

Isao Nambu,[1,2] Nobuhiro Hagura,[1,3] Satoshi Hirose,[1,4] Yasuhiro Wada,[2] Mitsuo Kawato[5] and Eiichi Naito[1,6]

[1]Center for Information and Neural Networks, National Institute of Information and Communications Technology, CiNet Building, 1-4 Yamadaoka, Suita, Osaka 565-0871, Japan

[2]Graduate School of Engineering, Nagaoka University of Technology, 1603-1 Kamitomioka, Nagaoka, Niigata 940-2188, Japan

[3]Institute of Cognitive Neuroscience, University College London, London, UK

[4]The Japan Society for the Promotion of Science, Tokyo, Japan

[5]ATR Computational Neuroscience Laboratories, Keihanna Science City, Kyoto, Japan

[6]Graduate School of Medicine and Graduate School of Frontier Biosciences, Osaka University, Suita, Osaka, Japan

Keywords: functional magnetic resonance imaging decoding, human brain, motor sequence, movement preparation

Edited by Sophie Molholm

Received 9 April 2015, revised 22 August 2015, accepted 1 September 2015

Abstract

Performing a complex sequential finger movement requires the temporally well-ordered organization of individual finger movements. Previous behavioural studies have suggested that the brain prepares a whole sequence of movements as a single set, rather than the movements of individual fingers. However, direct neuroimaging support for this hypothesis is lacking and, assuming it to be true, it remains unclear which brain regions represent the information of a prepared sequence. Here, we measured brain activity with functional magnetic resonance imaging while 14 right-handed healthy participants performed two types of well-learned sequential finger movements with their right hands. Using multi-voxel pattern analysis, we examined whether the types of the forthcoming sequence could be predicted from the preparatory activities of nine regions of interest, which included the motor, somatosensory and posterior parietal regions in each hemisphere, bilateral visual cortices, cerebellum and basal ganglia. We found that, during preparation, the activity of the contralateral motor regions could predict which of the two sequences would be executed. Further detailed analysis revealed that the contralateral dorsal premotor cortex and supplementary motor area were the key areas that contributed to the prediction consistently across participants. These contrasted with results from execution-related brain activity where a performed sequence was successfully predicted from the activities in the broad cortical sensory-motor network, including the bilateral motor, parietal and ipsilateral somatosensory cortices. Our study supports the hypothesis that temporary well-organized sequences of movements are represented as a set in the brain, and that preparatory activity in higher-order motor regions represents information about upcoming motor actions.

Introduction

Planning and generating complex motor skills requires the elaborate temporal and ordinal arrangement of motor elements. A typical example of this dexterous motor behaviour is sequential finger movement, such as performed by pianists who can quickly and smoothly play complicated patterns of musical notes. This ability is possible because our brains prepare the movements in advance, and behavioural studies have suggested that this is achieved through neuronal representations of sequences as single sets, as opposed to discrete representations of each finger movement (Sakai *et al.*, 2003; Rhodes *et al.*, 2004).

However, direct evidence for this hypothesis from human neuroimaging studies is lacking, including any indication as to which brain regions are involved in preparing these types of motor sequences. In non-human primate studies, it has been shown that discharge of cells in motor areas [e.g. supplementary motor area (SMA)] shows a preference for the preparation of a particular order of multiple actions (Tanji, 2001). Previous neuroimaging studies have found that increased brain activations are observed in a wide range of sensory-motor-related regions, e.g. the primary motor, premotor, somatosensory and parietal cortices, basal ganglia and cerebellum (CB) (Shibasaki *et al.*, 1993; Sadato *et al.*, 1996; Catalan *et al.*, 1998; Harrington *et al.*, 2000; Bengtsson *et al.*, 2004; Bortoletto & Cunnington, 2010; Heim *et al.*, 2012). Despite this evidence,

Correspondence: Isao Nambu, [2]Graduate School of Engineering, as above.
E-mail: inambu@vos.nagoakaut.ac.jp
Eiichi Naito, [1]Center for Information and Neural Networks, as above.
E-mail: eiichi.naito@nict.go.jp

it is unclear whether increased activity in these regions actually represents information about a specific sequence.

Recently, a study using multi-voxel pattern analysis (MVPA) has shown that types of executed sequences can be predicted from the activity in these sensory-motor-related regions during movement execution (Wiestler & Diedrichsen, 2013), suggesting that the activity in these regions specifically represents a particular type of executed sequence. However, this execution-related activity can be contaminated with the motor commands that control the finger muscles, as well as corollary discharges and the reafferent feedback signal from the fingers; therefore, they may not purely represent the information of the sequence *per se*.

Hence, here we focus on the brain activation during the preparation period, when the actual motor commands and sensory signals are not contaminated. We measured brain activity with functional magnetic resonance imaging (fMRI) while 14 participants performed two different types of well-learned sequential finger movements. We tested whether MVPA applied on the preparatory brain activity of the sensory-motor-related regions can predict which of the two sequences will be executed after this period. Based on the previous findings described above, we hypothesize that preparatory activity in some of the above sensory-motor-related regions represents information about a specific sequence and we set nine regions of interest (ROIs): the motor, somatosensory and posterior parietal regions in each hemisphere, and bilateral CB, basal ganglia and visual cortices. We evaluated how accurately a type of sequential finger movement can be predicted from multi-voxel patterns of these ROIs before its execution. We also performed the same analysis for the activities of these regions during execution, and compared this result with that obtained from the analysis for the movement preparation.

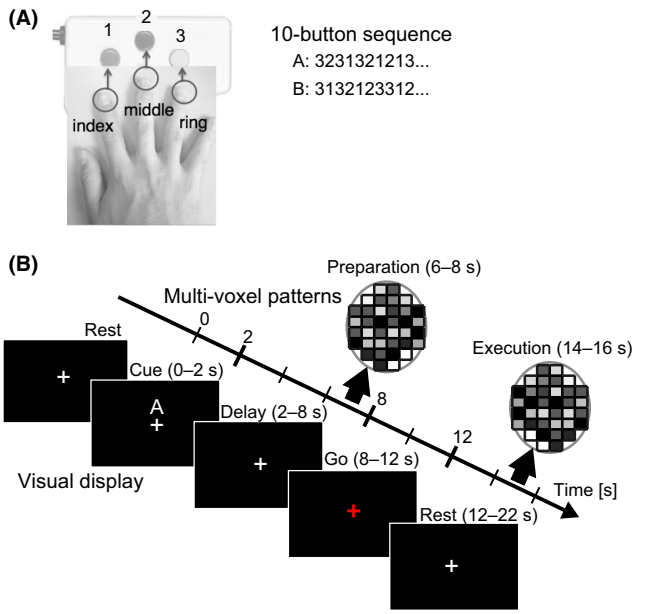

FIG. 1. Experimental design. (A) Task: a sequential button-press task using the right index (1), middle (2) and ring (3) fingers. Two different sequences (A and B) were prepared for each participant. For each assigned sequence, a fixed pattern of 10 button presses (e.g. 3-2-3-1-3-2-1-2-1-3 in the case of A) was repeated twice (20 button presses). (B) An example of a target trial. When the 'A' cue was presented, participants were required to immediately prepare the sequential finger movement that corresponded to the 'A' cue. They then initiated the sequence when the fixation cross turned red (go signal) after a 6-s delay period. The functional volume obtained during the last 2 s of the delay period (i.e. 6–8 s after the onset of the cue in the target trial) was used for the MVPA as the preparation volume. The volume obtained from 2 s after the end of the go signal was defined as the execution volume (14–16 s after the onset of the cue).

Materials and methods

Participants

Fourteen right-handed healthy volunteers participated in the experiment (12 male and two female; mean age 27.3 years). The study was approved by the Institutional Review Board of ATR (Kyoto, Japan), where the current study was conducted. All participants gave written informed consent, and the experiment was carried out according to the principles and guidelines of the Declaration of Helsinki.

Magnetic resonance imaging measurement

The participants were scanned in a 3.0-T magnetic resonance imaging scanner (MAGNETOM Verio, Siemens, Munich, Germany) with a 12-channel head matrix coil in the ATR Brain Activation Imaging Center (Kyoto, Japan). T1-weighted anatomical images [magnetisation-prepared rapid gradient-echo (MP-RAGE)] and functional T2*-weighted echo-planar images (64×64 matrix; pixel size, 3.0×3.0 mm^2; flip angle, 80°; echo time, 30 ms) were measured using a gradient echo-planar imaging sequence. Functional volumes were collected every 2 s (repetition time, TR, 2000 ms) and comprised 30 4.0-mm-thick slices with 1.0-mm interslice gaps. The whole brain was within the field of view (192×192 mm^2).

Experimental procedure

Prior to the fMRI experiment, the participants practiced two types of button-press sequences using their right index, middle, and ring fingers. In each sequence, a pattern of 10 button presses was repeated (i.e. each sequence consisted of 20 button presses; Fig. 1A). We assigned a different pair of patterned sequences to each participant. The two sequences assigned to each participant always started with the same finger and comprised the same number of button presses for each finger. This was done to eliminate the possibility that decoding a sequential finger movement could be achieved merely by the difference of the finger used in the very first button press or by the difference in the number of uses of each finger between two sequences (for details, see Appendix S1). Before the fMRI experiment (on a different day from an fMRI scanning day), the participants were trained for about 1.5 h until they were able to complete a sequence within 4 s. After the training, all participants reported that they had memorized the two sequences.

In the fMRI experiment, the participants rested comfortably in a supine position in the scanner. They were instructed not to generate unnecessary body movements and to keep gazing at a white fixation cross presented on the screen during the experiment (Fig. 1B). Visual instructions (the fixation cross and visual cues) were projected on the centre of a screen in the scanner, and the participants viewed them through a mirror located just in front of their eyes. These instructions were made using MATLAB (The Mathworks Inc., Natick, MA, USA) and Psychtoolbox (version 3.0; http://psychtoolbox.org/). The participants' right hands were placed on a magnetic resonance imaging-compatible button device (HHSC-1x4-D, Current Designs Inc., Philadelphia, PA, USA) located beside their bodies.

Each participant completed nine experimental runs. Each run was composed of 18 trials with 10-s intertrial intervals. Each trial started

with the appearance of a visual cue ('A' or 'B') that indicated which of the two sequences the participant should perform. The cues were displayed just above the fixation cross for 2 s (cue period), and the participants were asked to immediately prepare the instructed sequence.

There were two types of trials: 12 target trials and six randomly interleaved catch trials. In the target trials, we set a 6-s delay period after the offset of the visual cue. In the catch trials, the delay period was shorter, i.e. 0, 2, or 4 s. In both types of trials, the participants were required to initiate the movement as quickly as possible and to complete it within 4 s (execution period) when the colour of the fixation cross turned red (go signal) after the delay period. The catch trials were set to encourage participants to complete the preparation during the cue period. If they did not, they would not be able to initiate the movement quickly enough (i.e. in catch trials).

Each run also included an 18-s rest period before the first trial and another 10-s rest period after the last trial. Each run lasted for 400 s, and 200 functional volumes were collected per run.

Analysis

Functional magnetic resonance imaging data pre-processing

All fMRI analyses were conducted using MATLAB. The first five functional volumes in each run were excluded from the analysis to allow for magnetization equilibrium. The remaining volumes were realigned to correct head movements and co-registered to each participant's anatomical image using SPM5 software (Wellcome Trust Centre for Neuroimaging, University College London; http://www.fil.ion.ucl.ac.uk/spm/). A temporal high-pass filter (Butterworth filter with a cut-off frequency of 128 s) was applied to the data obtained in each run to remove low-frequency drift.

Functional magnetic resonance imaging univariate analysis

First, we performed conventional voxel-by-voxel univariate analysis using SPM5 for voxels in the whole brain. This was performed to confirm previous findings that brain activation increases in a wide range of sensory-motor-related regions during movement preparation and execution (see Introduction), and to validate our definition of ROIs for MVPA (see below).

The pre-processed data were spatially normalized into the Montreal Neurological Institute (MNI) standard brain coordinates and spatially smoothed with an 8-mm full width at half-maximum isotropic Gaussian kernel. We first fitted a linear regression (general linear) model to the data obtained from each participant. We had two conditions of interest in each experimental run, i.e. preparation and execution conditions. The preparation and execution conditions were separately modelled by boxcar functions representing a 2-s cue period and a 4-s execution period, respectively. These boxcar models were convolved with the canonical haemodynamic response function in SPM5. We also included the head motion parameters estimated in the realignment procedure as regressors in each run to minimize the effects of head motion artefacts. As the purpose of this analysis was to see general features of brain activity during preparation and execution, we did not distinguish between the two (A and B) types of sequential finger movement.

Then, to accommodate interparticipant variability, the images representing preparation-related and execution-related brain activity obtained from all participants were entered into a random effect group analysis with a one-sample *t*-test (13 degrees of freedom) (Friston *et al.*, 1999). A voxel-wise threshold of $T > 3.85$ ($P < 0.001$, uncorrected) was used to generate a cluster image. We evaluated the significance of brain activations in terms of their spatial extent (cluster-level $P < 0.05$) (Friston *et al.*, 1994).

Functional magnetic resonance imaging multi-voxel pattern analysis

We conducted an MVPA to elucidate whether preparatory brain activity represented sequential information about finger movements (Kamitani & Tong, 2005; Haynes & Rees, 2006; Wiestler & Diedrichsen, 2013). In this analysis, a multi-voxel pattern 'classifier' was trained through a supervised classification algorithm with a training dataset, which was composed of pairs of the multi-voxel patterns and their corresponding labels (i.e. type of sequence). After training the classifier, its performance was evaluated by how accurately the trained classifier could predict the label from novel multi-voxel patterns that were not included in the training (test dataset). For the classification algorithm, we used sparse logistic regression (SLR) (Yamashita *et al.*, 2008; http://www.cns.atr.jp/~oyamashi/SLR_WEB.html), which can automatically select the voxels and achieve higher classification accuracy from high-dimensional features without prior dimensional reduction (Miyawaki *et al.*, 2008; Yamashita *et al.*, 2008). An advantage of this analysis is that information represented as small differences in brain activity can be magnified by applying optimal weights to the multiple voxels. Thus, this analysis is suitable for assigning a brain activity pattern to each sequence, especially in the present situation where the difference in preparatory blood oxygenation level-dependent signal between the two highly similar sequences is likely to be subtle.

We set nine ROIs: the left (contralateral) and right (ipsilateral) motor regions (L-MOTOR, R-MOTOR), which are primarily involved in the planning and execution of actions for both contralateral and ipsilateral hands (Hoshi & Tanji, 2007; Nachev *et al.*, 2008; Kalaska, 2009); somatosensory regions (L-SS, R-SS), which mainly process somatosensory feedback of contralateral hand movements (Eickhoff *et al.*, 2008); posterior parietal cortices (L-PPC, R-PPC), which are generally involved in attention, integration of different sensory information and generation of abstract motor intention, and which are activated for both contralateral and ipsilateral movements (Culham & Valyear, 2006; Andersen & Cui, 2009); the bilateral basal ganglia, regions especially related to the control of both contralateral and ipsilateral movements (Alexander *et al.*, 1986); and the bilateral CB, related to voluntary control of limb movements and internal model formation (Manto *et al.*, 2011; Koziol *et al.*, 2014). In addition to these sensory-motor-related areas, we also used the bilateral visual areas (VIS) as control ROIs (Grill-Spector & Malach, 2004). Each ROI was defined based on cytoarchitectonic probability maps (SPM Anatomy toolbox v1.8; Eickhoff *et al.*, 2005). We selected all of the voxels that had non-zero probability in the probability map to include as many voxels as possible. The L-MOTOR and R-MOTOR included the primary motor cortex (areas 4a and 4p) and the secondary motor areas (area 6). The L-SS and R-SS included areas 1, 2, 3a and 3b of each hemisphere. The L-PPC and R-PPC included the superior (areas 5L, 5M, 5 Ci, 7A, 7PC, 7M and 7P) and inferior parietal cortices (areas PFop, PFt, PF, PFm, PFcm, PGa and PGp) as well as intraparietal regions (hIP1, hIP2 and hIP3). For the CB, all of the cerebellar regions contained in the SPM anatomy toolbox were included. The VIS included the bilateral VIS (areas V1, V2, V3v, V4 and V5). As the current toolbox did not provide any anatomical information for basal ganglia, the basal ganglia were created using a combined mask image from the ATAG atlas (http://www.nitrc.org/projects/atag; Keuken *et al.*, 2014). This included the striatum, globus pallidus,

red nucleus, substantia nigra and subthalamic nucleus in both hemispheres (Nonlinear_combined_masks_threshold033.nii.gz). All ROIs were defined in MNI standard brain coordinates (see Fig. S1 for the anatomical location of ROIs in the standard brain), and then transformed back into individual brain coordinates.

The time-course data of the fMRI signals without normalization and smoothing were extracted from every voxel in each ROI for each participant. The values of each voxel were then normalized by setting the mean value of the time-course data in each run to 100. Finally, the functional volume obtained during the last 2 s of the delay period in target trials (i.e. 6–8 s after the onset of the cue; preparation volume) was chosen and used for the classification analysis. Note that, considering the haemodynamic delay, this volume probably reflects preparatory activity begun after the cue was presented, which corresponds to the preparation condition used in the univariate analysis. For the execution, we used the volume obtained from 2 s after the end of the execution (i.e. 14–16 s after the onset of the cue; execution volume) (Fig. 1B). Catch trials were not included in the analysis because of the potential for contamination by execution-related activity or movement artefacts. We chose these volumes because they were most likely to contain signals associated with neuronal motor preparation and execution processes within the cue period and execution period, respectively. Note that these volumes were obtained during the periods where no actual movement was performed, and that the preparation volume was obtained before movement initiation. Thus, we could extract brain activity purely derived from movement preparation without contamination from movement artefacts or execution-related activity. Trials in which a participant pressed an incorrect button within the first two button presses in a sequence were excluded from the analysis (see Results) because, in this case, the movement was presumably not well prepared, or the participant might have prepared the wrong sequence. After excluding error trials, the number of trials for each sequence was balanced to avoid any bias in the following classification analysis.

To evaluate the accuracy of the classification, we performed leave-one-run-out cross-validation for each ROI in each participant. The classifier was trained using the training dataset obtained from eight out of nine runs, and the accuracy was evaluated in the trials of the remaining run (test dataset). This procedure was performed for all nine possible combinations of the training and test datasets. The mean accuracy across these nine combinations was regarded as the performance that was evaluated by the cross-validation. Before classifier training in each of the nine validation folds, we normalized the voxel values, i.e. voxel values in the training dataset were transformed into z-scores and the mean and SD of each voxel in the training dataset were used to normalize the voxel values in the test dataset (SLR toolbox option mean_mode: 'each'; scale_mode: 'stdeach'; norm_sep: 0).

We evaluated the statistical significance of the mean accuracy across the participants using a non-parametric permutation test (Stelzer *et al.*, 2013). In this test, we first performed permutations of the labels within a run, and calculated the accuracies for each participant using the cross-validation. By repeating this permutation and calculation of the accuracy 100 times, we obtained a pool of chance accuracies at the single participant level. We then calculated group chance accuracies (mean of chance accuracies across participants) for 10^5 times using a bootstrap method, and obtained empirical chance distributions of the mean accuracy (Stelzer *et al.*, 2013). The statistical significance of the mean accuracy was tested using this distribution for each ROI. To correct for multiple comparisons of the nine ROIs, we applied the false discovery rate method on *P*-values (false discovery rate threshold, $q < 0.05$, nine ROIs) (Benjamini & Hochberg, 1995). This statistical test was performed for preparation-related and execution-related volumes separately.

Mapping the location of relevant voxels

While training the classifier, SLR automatically selects the most informative voxels for the classification (for details, see Yamashita *et al.*, 2008), which, in our case, are the voxels that are most informative in discriminating the two sequences. By evaluating the consistency of the anatomical locations of selected voxels across participants, we can specify the detailed anatomical location of the key brain regions that uniquely represent each of the two types of sequential movements. To this end, we analysed the spatial distribution of the selected voxels within each of the ROIs, where we found significant above-chance classification accuracy (L-MOTOR for the preparation period; L-MOTOR, R-MOTOR, L-SS, R-SS, L-PPC, R-PPC and CB for the execution period; see Results). The procedures described below were applied to the results from each ROI separately.

We first identified the voxels that were selected by SLR in at least one of the nine validation folds for each participant. Next, the locations of the selected voxels were mapped onto the MNI template brain (spatial normalization; voxel size, $3.0 \times 3.0 \times 3.0$ mm^3), and the image representing the selected voxels in the template brain was created. This was a binary image in which we assigned a value of 1 to the selected voxel and a value of 0 to the non-selected one. We then smoothed this image of each participant by regarding the 26 neighbouring voxels surrounding each of the selected voxels (i.e. voxels that shared a face, an edge or a corner with the selected voxel were also assigned a value of 1). This procedure was performed to compensate for the slight differences across participants in the spatial locations of the selected voxels, which could be caused by limitations of the spatial normalization or the subtle individual differences in the relationship between the anatomical structure and its imposed brain function.

Then, to statistically evaluate the spatial consistency of the selected voxels across participants, we computed a voxel consistency index (VCI) for each selected voxel. This index was defined based on the number of participants (i.e. in how many participants a voxel was consistently regarded as the selected voxel) and its maximum value was 14. We adopted a voxel-shuffling analysis to empirically evaluate the null distribution of the VCI (Stelzer *et al.*, 2013), under the null hypothesis that 'the voxels were randomly selected.' First, we randomly shuffled the locations of the selected voxels in each participant. Next, the image representing 'shuffled selected voxels' was spatially normalized and smoothed using the same procedures as described above. These were performed for each participant. Then, using the images obtained from all participants, we calculated the 'random' VCI for each voxel. This shuffling analysis was repeated 1000 times, and the distribution of the random VCI was obtained (see Results). For example, in the case of preparation-related volume for L-MOTOR, this ROI included 6939 voxels (after smoothing), and eventually 6 939 000 random VCI values were obtained. The upper 5% of this distribution (one-tailed) was adopted as the voxel-wise threshold ($P < 0.05$). Finally, the spatial extent of voxels (cluster size) with above voxel-wise threshold VCI was also evaluated. To this end, we first identified the clusters from the original VCI image and 1000 'random' VCI images by using the 26-neighbouring connectivity scheme; two voxels were regarded as part of the same cluster if they shared a face, an edge or a corner (Poldrack *et al.*, 2011). The 'random' cluster-size distribution was then estimated from the cluster size data obtained in 1000 'random'

VCI images. For each identified cluster from the original VCI image, we evaluated whether its size was larger than the upper 5% point of the 'random' cluster-size distribution (with a multiple comparisons test using the false discovery rate method; $q < 0.05$; Benjamini & Hochberg, 1995).

Results

Behavioural results

The participants' incorrect button press (at least one within the first two button presses) was 2.4 ± 1.2% (mean ± 95% confidence interval across participants) of all of the trials, indicating that the participants were successful in preparing the instructed movements in almost all of the trials. In addition, the participants did not initiate the movement before the appearance of the go signal in any of the trials. Thus, the preparation-related volume probably reflected the activity related to movement preparation without contamination from movement artefacts or brain activation related to movement execution.

Results of univariate analysis

In the conventional voxel-by-voxel univariate analysis, we found that broad brain regions were recruited both during preparation and execution (Fig. 2). In particular, during preparation (Fig. 2A), brain activity increased in the contralateral and ipsilateral motor, somatosensory and superior and inferior parietal regions, which corresponded to L-MOTOR, R-MOTOR, L-SS, R-SS, L-PPC and R-PPC. We also found an increase in brain activity in the VIS, CB and basal ganglia ROIs.

During execution (Fig. 2B), the contralateral sensory-motor activities became more robust (L-MOTOR and L-SS; left panel in Fig. 2B). Activations of the contralateral posterior parietal (L-PPC), ipsilateral sensory, motor and posterior parietal cortices (R-MOTOR, R-SS and R-PPC) were observed as well as CB and VIS. Eventually, we found an increase in brain activity in all nine pre-defined ROIs during both preparation and execution. Details of the univariate results are tabulated in Table S1. Thus, the present brain activations observed during preparation and execution were in good agreement with those reported in previous studies (see Introduction), which ensures the validity of our pre-defined ROIs.

Results of multi-voxel pattern analysis for each region of interest

Despite the increase of brain activity in broader regions during sequence preparation (Fig. 2A), the MVPA for the preparation volume revealed that the prediction accuracy in L-MOTOR was the only region that was significantly greater than chance level after correcting for multiple comparisons ($P < 0.0001$; mean ± 95% confidence interval: 56.7 ± 3.3%; Fig. 3).

In contrast, when we analysed the execution volume (Fig. 3), significantly higher prediction accuracies ($P < 0.05$, corrected) were observed in L-MOTOR (56.9 ± 4.0%, $P < 0.0001$), R-MOTOR (56.7 ± 3.2%, $P < 0.0002$), L-SS (54.3 ± 3.2%, $P < 0.007$), R-SS (56.5 ± 3.7%, $P < 0.0001$), L-PPC (56.3 ± 4.4%, $P < 0.0002$), R-PPC (56.2 ± 4.3%, $P < 0.0004$) and CB (53.5 ± 3.2%, $P < 0.003$), which is generally in line with previous reports (Wiestler & Diedrichsen, 2013).

Mapping the voxels contributing to the prediction

Next, we evaluated the spatial distribution of relevant voxels in each ROI, from which we achieved significant prediction accuracy (Fig. 3). In the analysis of the preparation, L-MOTOR was the only ROI where a significant prediction accuracy was obtained (Fig. 3). In this ROI, we found two clusters of relevant voxels (Fig. 4A, Table 1). First, the largest cluster was identified in the medial-wall motor regions of cytoarchitectonic area 6 [MNI coordinates of the

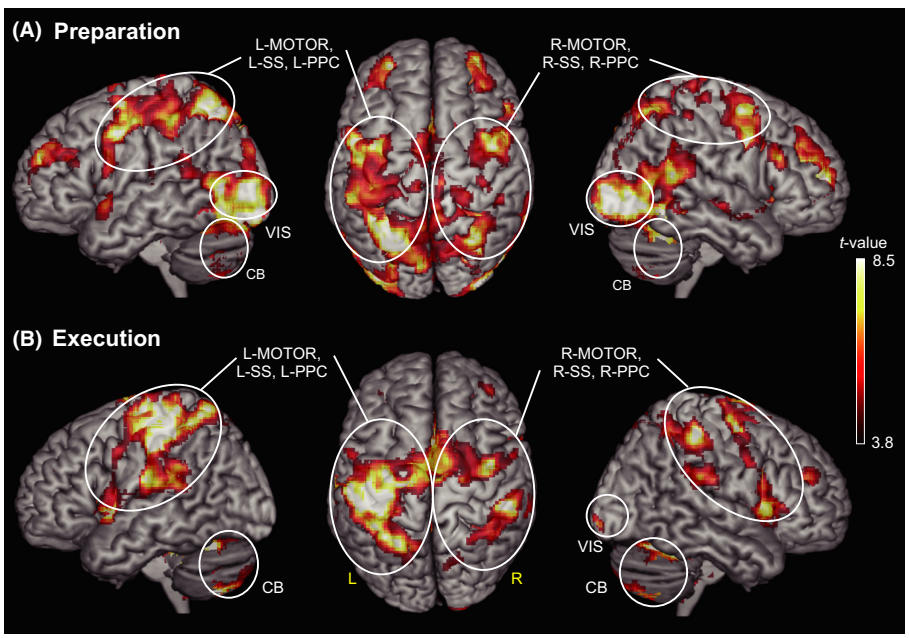

FIG. 2. Brain regions active during preparation (A) and execution (B). Each white circle roughly indicates activations in the pre-defined ROI for MVPA. Cluster level threshold $P < 0.05$ was applied (77 voxels for preparation and 56 voxels for execution). Each image was created using MRIcron software (http://www.mccauslandcenter.sc.edu/mricro/mricron/).

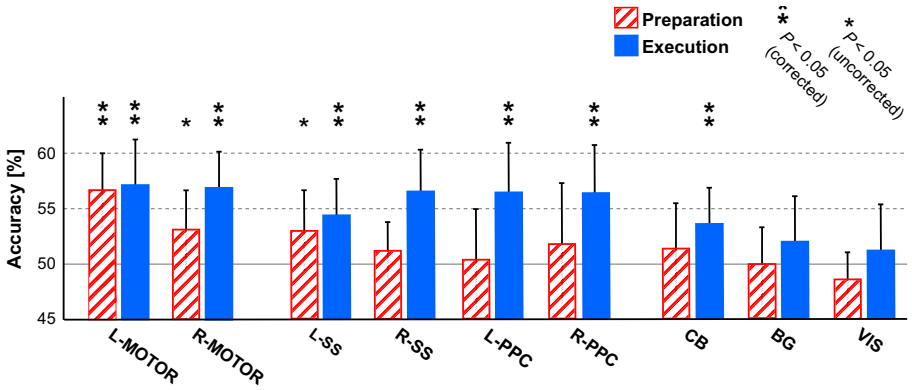

FIG. 3. Mean prediction accuracy across participants in each ROI. Accuracies obtained from the preparation and execution volumes are shown, respectively. The grey horizontal solid line indicates the chance level of prediction for binary classification (50%). Error bars indicate 95% confidence interval of means across participants. * $P < 0.05$ without correction for multiple comparisons; ** $P < 0.05$ after correction of multiple comparisons (false discovery rate) for nine ROIs. BG, basal ganglia.

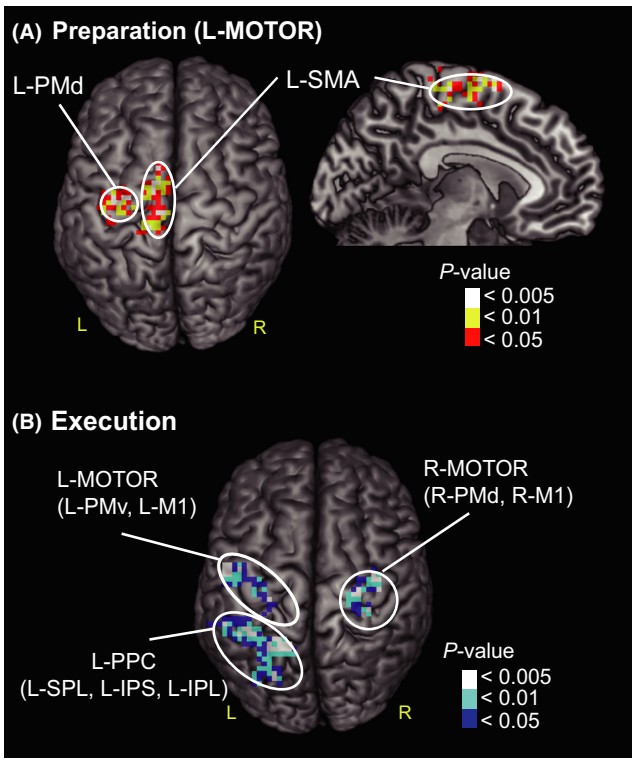

FIG. 4. Spatial locations of the relevant voxels during the preparation period (A) and execution period (B). The relevant voxels were superimposed on the surfaces of the template brain images using MRIcron software for display purposes. (A) Results from preparation volume. The clusters of relevant voxels were located in the SMA and PMd. The red, yellow and white (grey, light grey and white in the printed version) indicate voxels having a VCI of 10, 11 and 12, which corresponds to $P < 0.05$, $P < 0.01$ and $P < 0.005$, respectively. (B) Results from execution volumes. A cluster was found in each of the L-MOTOR, R-MOTOR and L-PPC. The blue, cyan and white (grey, light grey and white in the printed version) indicate voxels having a significant VCI of 10, 11 and 12 in L-MOTOR and R-MOTOR, and of 8, 9 and 10 in L-PPC, which corresponds to $P < 0.05$, $P < 0.01$ and $P < 0.005$, respectively. The details of cluster information and VCI threshold are listed in Table S2. IPL, inferior parietal lobule; IPS, intraparietal sulcus; M1, primary motor cortex; PMv, ventral premotor cortex; SPL, superior parietal lobule.

TABLE 1. Clusters of relevant voxels during preparation and execution periods

ROI	No. of voxels*	MNI coordinates of peak voxel†			VCI in peak voxel	Anatomical location of peak voxel
		x	*y*	*z*		
Preparation						
L-MOTOR	123	−6	−21	66	13	SMA
	90	−36	−15	54	13	PMd
Execution						
L-MOTOR	92	−51	−9	45	13	PMv
R-MOTOR	98	36	−12	54	13	PMd
L-PPC	221	−21	−48	54	12	SPL

*After cluster-level multiple comparison correction ($P < 0.05$, corrected with false discovery rate method). †Peak voxel was defined as the voxel having maximum VCI in the ROI. PMv, ventral premotor cortex; SPL, superior parietal lobule.

peak voxel (*x*, *y*, *z*): (−6, −21, 66)], which corresponds to the SMA (SMA-proper; Roland & Zilles, 1996). This cluster was located in the anterior and posterior parts of the SMA. We also found a cluster in the pre-central sulcus region [MNI coordinates of the peak voxel: (−36, −15, 54)], which was located in the lateral superior aspect of the pre-central sulcus (cytoarchitectonic area 6), and is probably the dorsal premotor cortex (PMd) (Picard & Strick, 2001).

As for execution, we performed the same analysis for the seven ROIs: L-MOTOR, R-MOTOR, L-SS, R-SS, L-PPC, R-PPC and CB (Fig. 3). We found one cluster in each of L-MOTOR, R-MOTOR and L-PPC (Fig. 4B, Table 1). No significant clusters were identified in the other ROIs (L-SS, R-SS, R-PPC and CB). In L-MOTOR, a significant cluster was located in the lateral part of the pre-central sulcus and the posterior part of the cluster reached to the anterior bank of the central sulcus [MNI coordinates of the peak voxel: (−51, −9, 45)]. Most of the voxels in this cluster were probably located in the ventral premotor cortex and primary motor cortex (Picard & Strick, 2001). In R-MOTOR, a cluster was found in the rostral part of the pre-central gyrus, which was probably associated with the PMd and primary motor cortex. In L-PPC, the relevant voxel cluster was located around the intraparietal sulcus and its rostral and dorsal parts were extended to the middle of the superior and inferior parietal lobules, respectively.

Discussion

We found that brain activity increased in broad regions during the preparation period (Fig. 2A), as has been previously reported (see Introduction). However, the MVPA (SLR) revealed that the type of sequential finger movement could be predicted only from the preparatory brain activity in the contralateral motor regions (L-MOTOR; Fig. 3). The important voxels that consistently contributed to the prediction across participants were identified in the contralateral SMA and PMd (Fig. 4A). These results indicate that preparatory motor programmes for sequential finger movements in these regions are shaped as a single unit and can specify the type of forthcoming movement.

Methodological considerations of the significant multi-voxel pattern analysis result and neuronal representation of sequences

During the preparation period, were the participants planning the sequence of the finger movements? Many behavioural studies have supported the hypothesis that sequential finger movement is encoded as a set, rather than discretely preparing each individual finger movement (for review, see Rhodes *et al.*, 2004). Also, in the present study, the participants intensively trained both types of sequences prior to the experiment, and they were able to perform long sequences within a short period of time (20 finger movements within 4 s). When we checked the shortening of the interkey intervals of the finger movement in the course of learning, which is one of the indicators of the formation of the sequential finger movement (Wymbs & Grafton, 2013), a significant reduction of the interkey interval was observed ($P < 0.02$) after the training (Appendix S3). Thus, these behavioural data suggest that the brain has acquired an internal model for each type of sequential finger movement through this intensive training and probably prepared the whole finger movement sequence as a set of actions, rather than as the movements of each individual finger, allowing the participants inside the scanner to generate this motor programme in a feedforward manner (Grafton *et al.*, 2008).

Next, was it really the information of the forthcoming sequence that the classifier relied on, to significantly predict the sequence type from the activity pattern in the motor areas? In the present study, we instructed a sequence to be executed by displaying either 'A' or 'B' during the cue period. Therefore, there is a possibility that the non-motor component, such as visual processing of the cue or the visual imagery, contributed to our significant classification of sequence in the motor areas. However, even when we analysed the activity in the VIS, which is primarily involved in the visual processing and visual imagery (Grill-Spector & Malach, 2004; Stokes *et al.*, 2009), the prediction accuracy did not exceed chance level (Fig. 3). As it is unlikely that the higher-order motor regions, such as the SMA and PMd, are more deeply involved in visual processing than the VIS, the difference in visual features may not explain the above-chance prediction achieved in L-MOTOR. We can also rebuff the view that movement artefacts (bodily movement) contributed to the prediction, because the prediction was made based on the brain activity during the period in which no physical movement was involved. Likewise, muscle activity during preparation did not contribute to the classification. In an additional experiment outside the magnetic resonance imaging scanner, we confirmed that, even though subtle activities in finger muscles were observed during preparation, these activities did not differ between two sequences (see Appendix S2). Thus, the muscle activity during preparation could not specify the type of forthcoming sequential finger movement.

Finally, in our experimental design, each participant always started each sequence with the same finger, and the number of button presses assigned to each finger was identical between the two sequences (see Appendix S1). Because of this procedure, the decoding process before the movement would not be able to differentiate the sequences if each elementary movement was planned separately. Therefore, we believe that the information used for the MVPA is the information about the sequence itself.

Differences between preparation and execution

One interesting result is that it was only from the contralateral motor regions that a type of forthcoming movement could be predicted during preparation (Fig. 3). This result contrasts with the finding that the type of movement could be predicted from execution-related brain activity not only in the contralateral motor regions but also in the ipsilateral motor regions, bilateral somatosensory cortices, bilateral parietal cortices and CB (Fig. 3). Together with the finding that an increase of brain activation was observed in these regions during both preparation and execution (Fig. 2), these results indicate that, although similar brain regions are recruited for both preparation and execution of sequential finger movement, the neuronal processing in the brain may be qualitatively different between these periods.

In general, during execution, the brain processes rich veridical sensory-motor information directly associated with actually executed movements, i.e. the motor commands sent to muscles, their associated corollary discharges and the sensory feedback of the performed movement (Evarts, 1981). This is likely to be one reason why two types of sequential finger movement could be predicted from the activity in a wide range of sensory-motor networks during execution (Fig. 3).

In contrast, the types of sequential finger movements could be predicted only from the activity in the contralateral motor regions during preparation (Fig. 3), although brain activity increased in a wide range of brain regions during this period (Fig. 2A). This finding can be better explained as follows. During preparation, the brain has planning-level information (Wise, 1985; Hoshi & Tanji, 2007). Some have proposed that, when motor sequences are planned, each elementary motor programme (in the lower level) is combined and processed as a set in higher-level brain regions (Rhodes *et al.*, 2004). Considering this hierarchical process, the planning-level information for a sequence is probably formed in such a way that it can specify a type of forthcoming movement only at the level of higher-order motor areas (SMA and PMd). However, the other brain regions recruited during preparation may process partial aspects of the plan or different aspects of the motor command, i.e. the effector to be used or the timing control of initiation of the movement, which may include little or no information specifying the type of sequence. Of course, this claim needs to be supported in future studies.

Roles of the supplementary motor area and dorsal premotor cortex during preparation

Here, we focus on the specific roles of the SMA and PMd. As we discussed above, our results suggest the exclusive contribution of the SMA and PMd to neuronal processing for motor sequences, which contrasts with results that different motor areas (ventral premotor cortex and primary motor cortex) mainly contribute to prediction during execution (Fig. 4B). This view is supported by previous studies in which the disruption of neuronal computation in these

regions by magnetically stimulating the SMA or PMd increases errors and hampers the completion of upcoming sequential finger movements (Gerloff *et al.*, 1997; Wymbs & Grafton, 2013). Importantly, this deficit is apparent particularly when people perform complex and well-learned sequential movements.

We are of the opinion that the SMA and PMd play different roles during preparation. It has been shown in non-human primates that SMA cell discharge shows a preference for the preparation of a particular order of multiple actions, e.g. some cells fire only when monkeys prepare push-pull-turn movements in this particular order (Mushiake *et al.*, 1991; Tanji & Shima, 1994). In contrast, PMd seems to be involved in the selection of motor commands for a single action from multiple candidates and in the association between external cues and their corresponding actions (Wise, 1985; Cisek & Kalaska, 2005; Hoshi & Tanji, 2007). Based on these findings, in the current study where the participant performed highly complex sequential finger movement, we speculate as to the roles of the SMA and PMd as follows. After the presentation of an external cue ('A' or 'B'), the PMd might select an appropriate set of motor commands from the candidates, and the SMA may build up the particular type of sequence of finger movements (Kettner *et al.*, 1996; Tanji, 2001; Nachev *et al.*, 2008). If so, the difference between the SMA and PMd can be investigated by manipulating the difficulty of the sequence (e.g. sequence length or number of fingers to be used) (Gerloff *et al.*, 1997; Harrington *et al.*, 2000; Haaland *et al.*, 2004) or amount of learning (Cross *et al.*, 2007; Wiestler & Diedrichsen, 2013; Wymbs & Grafton, 2013; Langner *et al.*, 2014) in future studies.

Summary and perspectives

Our study demonstrates that the preparatory activity of human higher-order motor regions (SMA and PMd) contains information about the types of forthcoming sequential movements. From a methodological viewpoint, our study shows for the first time that such complex, elaborate motor actions can be non-invasively read out from the human brain before action execution. By combining our findings with recent advanced techniques such as brain-machine (computer) interfaces (Wolpaw *et al.*, 2002) or neurofeedback (deCharms, 2008; Shibata *et al.*, 2011), decoded information about complex motor behaviour can be used for improvements in the control of neural prostheses or the efficacy of neurorehabilitation for regaining complex motor functions for people with movement disorders.

Supporting Information

Additional supporting information can be found in the online version of this article:

Appendix S1. Assignment of two sequences for each participant.
Appendix S2. Experiment outside scanner.
Appendix S3. Behavioral testing of sequence encoding.
Table S1. Areas activated during preparation and execution in the univariate analysis.
Table S2. Relevant Voxel Information for each ROI.
Fig. S1. Anatomical location of ROIs

Acknowledgements

None of the authors have any conflicts of interest associated with this study, which was supported in part by the Global COE Program 'Center of Human-Friendly Robotics Based on Cognitive Neuroscience' of MEXT (to E.N.), 'Novel and Innovative R&D Making Use of Brain Structures' of MIC, 'Development of Network Dynamics Modeling Methods for Human Brain Data Simulation Systems' of NICT, 'Strategic Research Program for Brain Science' of AMED (to M.K.), the Research Fellowship of the JSPS for Young Scientists (238768 to S.H.), JSPS KAKENHI (26560303 to I.N., 25119001 and 26119535 to N.H., 24300051 to Y.W., 24000012 and 26120003 to E.N.), and a Marie Curie International Incoming Fellowship (to N.H.). The authors would like to thank Dr Matthew DeBrecht for his helpful comments on the early version of the manuscript and Yuka Furukawa for technical support.

Abbreviations

CB, cerebellum; fMRI, functional magnetic resonance imaging; L-MOTOR, left motor region; L-PPC, left posterior parietal cortex; L-SS, left somatosensory region; MNI, Montreal Neurological Institute; MVPA, multi-voxel pattern analysis; PMd, dorsal premotor cortex; R-MOTOR, right motor region; ROI, region of interest; R-PPC, right posterior parietal cortex; R-SS, right somatosensory region; SLR, sparse logistic regression; SMA, supplementary motor area; VCI, voxel consistency index; VIS, visual areas.

References

Alexander, G.E., Delong, M.R. & Strick, P.L. (1986) Parallel organization of functionally segregated circuits linking basal ganglia and cortex. *Annu. Rev. Neurosci.*, **9**, 357–381.
Andersen, R.A. & Cui, H. (2009) Intention, action planning, and decision making in parietal-frontal circuits. *Neuron*, **63**, 568–583.
Bengtsson, S.L., Ehrsson, H.H., Forssberg, H. & Ullén, F. (2004) Dissociating brain regions controlling the temporal and ordinal structure of learned movement sequences. *Eur. J. Neurosci.*, **19**, 2591–2602.
Benjamini, Y. & Hochberg, Y. (1995) Controlling the false discovery rate: a practical and powerful approach to multiple testing. *J. Roy. Stat. Soc. B*, **57**, 289–300.
Bortoletto, M. & Cunnington, R. (2010) Motor timing and motor sequencing contribute differently to the preparation for voluntary movement. *NeuroImage*, **49**, 3338–3348.
Catalan, M.J., Honda, M., Weeks, R.A., Cohen, L.G. & Hallett, M. (1998) The functional neuroanatomy of simple and complex sequential finger movements: a PET study. *Brain*, **121**(Pt 2), 253–264.
deCharms, R.C. (2008) Applications of real-time fMRI. *Nat. Rev. Neurosci.*, **9**, 720–729.
Cisek, P. & Kalaska, J.F. (2005) Neural correlates of reaching decisions in dorsal premotor cortex: specification of multiple direction choices and final selection of action. *Neuron*, **45**, 801–814.
Cross, E.S., Schmitt, P.J. & Grafton, S.T. (2007) Neural substrates of contextual interference during motor learning support a model of active preparation. *J. Cogn. Neurosci.*, **19**, 1854–1871.
Culham, J.C. & Valyear, K.F. (2006) Human parietal cortex in action. *Curr. Opin. Neurol.*, **16**, 205–212.
Eickhoff, S.B., Stephan, K.E., Mohlberg, H., Grefkes, C., Fink, G.R., Amunts, K. & Zilles, K. (2005) A new SPM toolbox for combining probabilistic cytoarchitectonic maps and functional imaging data. *NeuroImage*, **25**, 1325–1335.
Eickhoff, S.B., Grefkes, C., Fink, G.R. & Zilles, K. (2008) Functional lateralization of face, hand, and trunk representation in anatomically defined human somatosensory areas. *Cereb. Cortex*, **18**, 2820–2830.
Evarts, E.V. (1981) Role of motor cortex in voluntary movements in primates. In *Handbook of Physiology, The Nervous System II*. American Physiological Society, Bethesda, MD, pp. 1083–1112.
Friston, K.J., Worsley, K.J., Frackowiak, R.S., Mazziotta, J.C. & Evans, A.C. (1994) Assessing the significance of focal activations using their spatial extent. *Hum. Brain Mapp.*, **1**, 210–220.
Friston, K.J., Holmes, A.P. & Worsley, K.J. (1999) How many subjects constitute a study? *NeuroImage*, **10**, 1–5.
Gerloff, C., Corwell, B., Chen, R., Hallett, M. & Cohen, L.G. (1997) Stimulation over the human supplementary motor area interferes with the organization of future elements in complex motor sequences. *Brain*, **120**(Pt 9), 1587–1602.
Grafton, S.T., Schmitt, P.J., van Horn, J.D. & Diedrichsen, J. (2008) Neural substrates of visuomotor learning based on improved feedback control and prediction. *NeuroImage*, **39**, 1383–1395.
Grill-Spector, K. & Malach, R. (2004) The human visual cortex. *Annu. Rev. Neurosci.*, **27**, 649–677.

Haaland, K.Y., Elsinger, C.L., Mayer, A.R., Durgerian, S. & Rao, S.M. (2004) Motor sequence complexity and performing hand produce differential patterns of hemispheric lateralization. *J. Cogn. Neurosci.*, **16**, 621–636.

Harrington, D.L., Rao, S.M., Haaland, K.Y., Bobholz, J.A., Mayer, A.R., Binderx, J.R. & Cox, R.W. (2000) Specialized neural systems underlying representations of sequential movements. *J. Cogn. Neurosci.*, **12**, 56–77.

Haynes, J.-D. & Rees, G. (2006) Decoding mental states from brain activity in humans. *Nat. Rev. Neurosci.*, **7**, 523–534.

Heim, S., Amunts, K., Hensel, T., Grande, M., Huber, W., Binkofski, F. & Eickhoff, S.B. (2012) The role of human parietal area 7A as a link between sequencing in hand actions and in overt speech production. *Front. Psychol.*, **3**, 534.

Hoshi, E. & Tanji, J. (2007) Distinctions between dorsal and ventral premotor areas: anatomical connectivity and functional properties. *Curr. Opin. Neurobiol.*, **17**, 234–242.

Kalaska, J.F. (2009) From intention to action: motor cortex and the control of reaching movements. *Adv. Exp. Med. Biol.*, **629**, 139–178.

Kamitani, Y. & Tong, F. (2005) Decoding the visual and subjective contents of the human brain. *Nat. Neurosci.*, **8**, 679–685.

Kettner, R.E., Marcario, J.K. & Port, N.L. (1996) Control of remembered reaching sequences in monkey. II. Storage and preparation before movement in motor and premotor cortex. *Exp. Brain Res.*, **112**, 347–358.

Keuken, M.C., Bazin, P.L., Crown, L., Hootsmans, J., Laufer, A., Müller-Axt, C., Sier, R., van der Putten, E.J., Schäfer, A., Turner, R. & Forstmann, B.U. (2014) Quantifying inter-individual anatomical variability in the subcortex using 7 T structural MRI. *NeuroImage*, **94**, 40–46.

Koziol, L.F., Budding, D., Andreasen, N., D'Arrigo, S., Bulgheroni, S., Imamizu, H., Ito, M., Manto, M., Marvel, C., Parker, K., Pezzulo, G., Ramnani, N., Riva, D., Schmahmann, J., Vandervert, L. & Yamazaki, T. (2014) Consensus paper: the cerebellum's role in movement and cognition. *Cerebellum*, **13**, 151–177.

Langner, R., Rottschy, C., Laird, A.R., Fox, P.T. & Eickhoff, S.B. (2014) Meta-analytic connectivity modeling revisited: controlling for activation base rates. *NeuroImage*, **99**, 559–570.

Manto, M., Bower, J.M., Conforto, A.B., Delgado-García, J.M., da Guarda, S.N.F., Gerwig, M., Habas, C., Hagura, N., Ivry, R.B., Mariën, P., Molinari, M., Naito, E., Nowak, D.A., Oulad Ben Taib, N., Pelisson, D., Tesche, C.D., Tilikete, C. & Timmann, D. (2011) Consensus paper: roles of the cerebellum in motor control—the diversity of ideas on cerebellar involvement in movement. *Cerebellum*, **11**, 457–487.

Miyawaki, Y., Uchida, H., Yamashita, O., Sato, M.A., Morito, Y., Tanabe, H.C., Sadato, N. & Kamitani, Y. (2008) Visual image reconstruction from human brain activity using a combination of multiscale local image decoders. *Neuron*, **60**, 915–929.

Mushiake, H., Inase, M. & Tanji, J. (1991) Neuronal activity in the primate premotor, supplementary, and precentral motor cortex during visually guided and internally determined sequential movements. *J. Neurophysiol.*, **66**, 705–718.

Nachev, P., Kennard, C. & Husain, M. (2008) Functional role of the supplementary and pre-supplementary motor areas. *Nat. Rev. Neurosci.*, **9**, 856–869.

Picard, N. & Strick, P. (2001) Imaging the premotor areas. *Curr. Opin. Neurobiol.*, **11**, 663–672.

Poldrack, R.A., Mumford, J.A. & Nichols, T.E. (2011) *Handbook of Functional MRI Data Analysis*. Cambridge University Press, New York.

Rhodes, B.J., Bullock, D., Verwey, W.B., Averbeck, B.B. & Page, M.P.A. (2004) Learning and production of movement sequences: behavioral, neurophysiological, and modeling perspectives. *Hum. Mov. Sci.*, **23**, 699–746.

Roland, P.E. & Zilles, K. (1996) Functions and structures of the motor cortices in humans. *Curr. Opin. Neurol.*, **6**, 773–781.

Sadato, N., Campbell, G., Ibáñez, V., Deiber, M. & Hallett, M. (1996) Complexity affects regional cerebral blood flow change during sequential finger movements. *J. Neurosci.*, **16**, 2691–2700.

Sakai, K., Kitaguchi, K. & Hikosaka, O. (2003) Chunking during human visuomotor sequence learning. *Exp. Brain Res.*, **152**, 229–242.

Shibasaki, H., Sadato, N., Lyshkow, H., Yonekura, Y., Honda, M., Nagamine, T., Suwazono, S., Magata, Y., Ikeda, A. & Miyazaki, M. (1993) Both primary motor cortex and supplementary motor area play an important role in complex finger movement. *Brain*, **116**(Pt 6), 1387–1398.

Shibata, K., Watanabe, T., Sasaki, Y. & Kawato, M. (2011) Perceptual learning incepted by decoded fMRI neurofeedback without stimulus presentation. *Science*, **334**, 1413–1415.

Stelzer, J., Chen, Y. & Turner, R. (2013) Statistical inference and multiple testing correction in classification-based multi-voxel pattern analysis (MVPA): Random permutations and cluster size control. *NeuroImage*, **65**, 69–82.

Stokes, M., Thompson, R., Cusack, R. & Duncan, J. (2009) Top-down activation of shape-specific population codes in visual cortex during mental imagery. *J. Neurosci.*, **29**, 1565–1572.

Tanji, J. (2001) Sequential organization of multiple movements: involvement of cortical motor areas. *Annu. Rev. Neurosci.*, **24**, 631–651.

Tanji, J. & Shima, K. (1994) Role for supplementary motor area cells in planning several movements ahead. *Nature*, **371**, 413–416.

Wiestler, T. & Diedrichsen, J. (2013) Skill learning strengthens cortical representations of motor sequences. *eLife*, **2**, e00801.

Wise, S.P. (1985) The primate premotor cortex: past, present, and preparatory. *Annu. Rev. Neurosci.*, **8**, 1–19.

Wolpaw, J.R., Birbaumer, N., McFarland, D.J., Pfurtscheller, G. & Vaughan, T.M. (2002) Brain-computer interfaces for communication and control. *Clin. Neurophysiol.*, **113**, 767–791.

Wymbs, N.F. & Grafton, S.T. (2013) Contributions from the left PMd and the SMA during sequence retrieval as determined by depth of training. *Exp. Brain Res.*, **224**, 49–58.

Yamashita, O., Sato, M.A., Yoshioka, T., Tong, F. & Kamitani, Y. (2008) Sparse estimation automatically selects voxels relevant for the decoding of fMRI activity patterns. *NeuroImage*, **42**, 1414–1429.